

# Interquark potential, susceptibilities and particle density of two color QCD at finite chemical potential and temperature

Maria-Paola Lombardo  
*Istituto Nazionale di Fisica Nucleare*  
*Laboratori Nazionali del Gran Sasso*  
*S.S. 17 bis Km. 18,910 I-67010 Assergi (AQ), Italy*  
*lombardo@lngs.infn.it*

## Abstract

We explore the phase diagram of SU(2) Lattice Gauge Theory with dynamical fermions in the temperature, mass, chemical potential space. We observe qualitative changes of the dependence of the particle density on  $\mu$  and  $T$ , which is compatible with that expected of a gas of free massless quarks  $n \propto \mu^3$  only for  $T \simeq T_c$ . At the onset for thermodynamics the interquark potential flattens at large separations, indicating enhanced fermion screening and the transition to a deconfined phase. Temporal and spatial Polyakov loops behave in different ways, the latter being nearly insensitive to the chemical potential. The rotation of the chiral condensate to a baryonic condensate, as inferred from the susceptibilities, might occur together with a reduction of its magnitude in the chiral limit, possibly leading to a critical temperature for diquark condensation smaller than the deconfinement temperature. We further assess the rôle of the chemical potential into the gauge dynamics by carrying out a partial quenched calculation. We speculate on the relevance, or lack thereof, of our findings to real QCD.

## I. INTRODUCTION

A so far unique possibility to study a gauge model at finite density is afforded by two color QCD, which can be studied via numerical simulations even at non-zero chemical potential. In our first paper [1] (hereafter HKLM) we have studied the model at zero temperature, presenting the first *ab initio* spectrum calculation at finite baryon density with full fermion feedback. Here we focus on the effect of temperature: we discuss the interplay of bulk thermodynamics observables, deconfinement and chiral symmetry by varying the chemical potential at different temperatures, and we contrast the nature of the phenomena along the temperature and density axes. Ultimately, we would like to understand the phase diagram of two color QCD, the nature of the critical lines separating the phases with different realisation of chiral symmetries and their interplay with the deconfinement and topological transitions. Finally, and ideally, we would also like to use some of the results on two color QCD to learn something about three color QCD. Clearly the present study, which addresses only a subset

of these issues on a small  $6^4$  lattice is just exploratory : we stress that even the “simple”  $\mu = 0$  limit, whose study was initiated many years ago in [2], has a number of interesting open problems [3].

A rich phenomenology at finite baryon density emerges from the analysis of model Hamiltonians with the same global symmetries as QCD [4]. For two colors the predictions of these more sophisticated studies reduce to those expected of qualitative reasoning and early calculations [5]. Simple models and qualitative reasoning, clearly, do not take fully into account details of the dynamics such as color forces and their temperature dependence: perhaps some of the lattice results can offer some quantitative control, and further insight into model studies, and, very optimistically, even the possibility of a first principle derivation of some of their relevant parameters (e.g. form factors). This provides a further motivation for this lattice study of two color QCD.

An overview of the parameter space explored by the numerical simulations is given in Section II, while the results for the quark-(anti)quark potential are presented in Section III. Section IV discusses the particle number, and the “nuclear matter phase”. Section V presents the data for the susceptibilities, contrasting the high density and high temperature behaviour. In Section VI we further assess the rôle of the chemical potential into the gauge dynamics by carrying out a partial quenched calculation, and present some speculative comments on the relationships of two and three color QCD. We close with a summing up and outlook. Some of the results of this paper have been briefly mentioned in [6].

## II. OVERVIEW OF THE PARAMETER SPACE

Using the same algorithm as in HKLM we studied the thermodynamics of the system on a  $6^4$  lattice at:

- $\beta = 1.3$ ,  $\mu = (0, .2, .6, .8)$ , mass = (.07, .05);
- $\beta = 1.5$ ,  $\mu = (0, .2, .6, .8, 1.0)$ , mass = (.1, .07, .05);
- $\mu = 0$ ,  $\beta = (1.3, 1.5, 1.7, 1.9, 2.1, 2.3)$ , mass = .1.

The chemical potential explores the range of interest, up to the lattice saturation, while the temperature ranges from  $T \simeq 0$  to  $T > T_c$ . By contrasting the results obtained at  $\beta = 1.5$  with those obtained at  $\beta = 1.3$  we shall study how the temperature effects the chemical potential dependence. By contrasting the results as a function of chemical potential with those obtained by varying the temperature we shall compare the nature of the high T and the high  $\mu$  transitions. Wherever available we rely on the results for condensates and susceptibilities obtained in HKLM.

Clearly to study the chemical potential dependence at different temperature we need to know in which phase we are in at  $\mu = 0$ . Our first task is then (approximately) locate the critical line in the  $\beta$ -mass plane. To this end we measured the mass dependence of the chiral condensate.

In Fig. 1 we show the chiral condensate as a function of the bare mass for different values of the chemical potential at  $\beta = 1.5$ . We note that, while a linear extrapolation from masses .1 and .07 would give a non-zero condensate, an extrapolation which uses masses .07 and .05

would suggest that chiral symmetry is already restored. In addition to that, for mass = .05 we observed a clear two state signal in the HMD history of the chiral condensate, which, to a lesser extent, was also visible at mass = .07. Fig. 1 should be considered together with the analogous one ( Fig. 3) of HKLM from which we inferred that the points  $\beta = 1.3$ , mass = .05 and .07 are in the phase where  $\langle \bar{\psi}\psi \rangle \neq 0$ . Assuming a first order chiral transition in  $\beta$  at  $m = 0$ , we would conclude that the chiral transition line in the  $\beta - m$  plane runs close to the points  $(\beta, m) = (1.5, .05), (1.5, .07)$ . We sketch such a line in Fig. 2, with the caveat that if the  $m = 0$  transition were instead second order, the line drawn in Fig. 2 would indicate a crossover. Given the exploratory nature of this study this distinction is immaterial. In the same Figure we also show the locations of the simulation points  $\beta = (1.3, 1.5)$ , and  $m = (.05, .07, .1)$ : by switching on the chemical potential we should be able to observe the effect of a finite density of quarks on a variety of dynamical situations, ranging from “very cold” (filled points), to “critical” (shaded points) to “hot” (open point). In addition to this, the line  $m = 0.1$  has been explored at  $\mu = 0$  for several  $\beta$ 's.

In Fig. 1 it is also shown the dependence of the chiral condensate on the chemical potential. As expected, when  $\mu$  is increased the chiral condensate extrapolates to zero in the chiral limit also for larger bare masses. We remind that, of course, this does not correspond to the restoration of the chiral symmetry as the chiral condensate will be rotated to a baryonic diquark one ( see the discussions in HKLM, and below, for more). Figs. 3 show the same  $\langle \bar{\psi}\psi \rangle$  data plotted as a function of the chemical potential. Again, the findings at this largest temperature should be contrasted with those obtained in HKLM which we reproduce for the reader's convenience in the upper part of the figure. At  $\beta = 1.3$ , mass = .07 we observe a rather sharp drop in the chiral condensate at  $\mu \simeq .3$ , close to the half the pion mass,  $m_\pi/2 \simeq .3$ . We also note that at  $\beta = 1.5$ ,  $m = .1$   $m_\pi = .8$ , and  $\mu \simeq m_\pi/2 \simeq .4$  lies somewhere in the crossover region as it should.

The overall observation resulting from Fig. 1 is that the density transition shows the expected softening at smaller masses and higher temperatures.

### III. QUARK-ANTIQUARK AND QUARK-QUARK INTERACTIONS

Although the results for  $\langle \bar{\psi}\psi \rangle$  look physical, and consistent with expectations, we would have obtained similar ones by use of the quenched approximation: we are not really observing qualitative, dynamical  $\mu$  effects. It is interesting to investigate the dynamics of the gauge fields, and to this end we measured the correlations  $\langle P(O)P^\dagger(z) \rangle$  of the zero momentum Polyakov loops, averaged over spatial directions. Remember that this quantity is related to the string tension  $\sigma$  via  $\lim_{z \rightarrow \infty} \langle P(O)P^\dagger(z) \rangle \propto e^{-\sigma z}$ .

Note that as  $P$  is a real quantity the Polyakov loop correlator defining the strength of the quark-quark interaction  $\langle P(O)P(z) \rangle / \langle P(0)^2 \rangle$  would be the same as the quark-antiquark one  $\langle P(O)P^\dagger(z) \rangle / \langle |P(0)|^2 \rangle$ . This would lead to the conclusion that the diquarks and mesons with the same spin and opposite parity are always degenerate, since their binding forces are the same. In principle this conclusion is limited to the heavy spectrum, however the numerical results presented in HKML support this point of view: mesons and diquarks seem to remain degenerate in SU(2) at any nonzero density, once the Fermi level shift is taken into account, producing four degenerate particles at large  $\mu$ .

We show the results for the Polyakov loop correlators in Fig. 4, where we compare the behaviour at various temperature (upper) with that at various chemical potentials (lower). We note that the trends with temperature and chemical potential are quite similar: in both cases we have signs of long range ordering, i.e. deconfinement. The gap between the plateaus having  $\mu = .4$  and  $\mu = .6$  in Fig. 3b suggests increased fermion screening and the passage to a deconfined phase. We have then a direct evidence of the effect of the chemical potential on the gauge fields.

Finally, we show (Fig. 5) the dependence of the Polyakov loop itself on the chemical potential, contrasted, in the lower part of the figure, with that of the spatial Polyakov loop. This suggests that the ordering effects of the chemical potential only affects the temporal direction. We should also note that some distinction between the behaviour of temporal and spacial Polyakov loop is also seen in the temperature dependence, and can be tentatively ascribed to an effect of the different boundaries for the fermion fields (periodic vs. antiperiodic) in space and time direction.

#### IV. THE NUCLEAR MATTER OF SU(2), AND A “NEW VACUUM”?

According to the standard wisdom for a chemical potential comparable with the baryon mass, baryons start to be produced thus originating a phase of cold, dense matter. For SU(2) baryons (diquarks) are bosons (as opposed to the fermionic baryons of real QCD). This has major implications on the physics of the dense phase. First, and obviously, the thermodynamics of (interacting) Bose and Fermi gases is different. In particular, it could be that the energetics favours the condensations of bosons. This would be revealed by a non-zero diquark condensate [5], which still breaks chiral symmetry, and should be reflected by different functional dependence of the particle density on  $\mu$  which can thus characterise the various phases.

In this exploratory study we just (try to) fit the data to a cubic spline, appropriate from free massless fermion at zero temperature, and try to infer from that the effect of temperature, and the possibility of a condensed diquark phase. In Figs. 6 we show the number density as a function of  $\mu$  for the two  $\beta$ 's values, with superimposed the fits described below.

Let us consider  $\beta = 1.5$  (our warmer lattice, close to  $T_c$ ) first: we note the following features. At small chemical potential there is a clear dependence on the bare mass, which is greatly reduced in the thermodynamical region. This could be ascribed to a loss of the dynamical mass. In the same region, the behaviour is close to  $\mu^3$  (the line connecting the point is the polynomial  $2.07\mu^3 - .01\mu^2 + .01$ ). We just note here that a simple, pure cubic term accommodates the data well suggesting a free quark gas – somewhat surprisingly, the contribution of the temperature term seems to be small [7]. At  $\beta = 1.3$  the situation is different. For  $\mu > \mu_c$ , we would expect diquark condensation. At the same time, we have observed long distance screening and deconfinement, so the behaviour might get closer to that of a cold phase of free quarks, which, however, is not supported by the data : as the diquark states appear to be bound (HKLM), their condensates can still influence the thermodynamics. The polynomial fits  $n(\mu) = .84\mu^3 + 1.27\mu^2 - .1$  for mass = .05,  $n(\mu) = 1.2\mu^3 + 0.5\mu^2 - .03$  for mass = .07 are not amenable to any simple interpretation. We might well expect a rather complicated “mixed” nuclear matter phase, with an admixtures

of diquark gas (which, if alone, would constitute a “pure” SU(2) nuclear matter), condensed diquarks, free quarks, perhaps characterised by both types of condensates (such mixed phases are also predicted by more detailed instanton studies [8]). A direct measure of diquark condensate should completely clarify this point [9]. A free massless quark phase, with complete restoration of chiral symmetry (i.e.  $\langle \bar{\psi}\psi \rangle = \langle \psi\psi \rangle = 0$ ) could be reached at even larger  $\mu$  – as this region is dominated by lattice saturation artifacts, improved/perfect actions [10] might be necessary to explore it.

## V. PARTICLE CONTENT AND CONDENSATION

Clearly to better understand the thermodynamics results shown above it is useful to assess the particle content of the model, together with their possible condensation. Remember that at  $\mu = 0$  the model has a lattice analogous of the Pauli–Gürsey symmetry mixing quarks and antiquarks which belong to equivalent representation. Main consequences are 1. the only discernable condensate is  $\langle qq \rangle^2 + \langle q\bar{q} \rangle^2$ , 2. the preferred direction of  $\chi SB$  is picked by the explicit mass term 3. the diquark condensate is a natural object which does not break any more symmetry than the ordinary condensate 4. there are massless baryons (diquarks). When  $\mu \neq 0$  the symmetry group is smaller, coincident with that of staggered fermions, and the number of Goldstone modes is reduced accordingly.

We refer to HKLM for more detailed discussions, and just reproduce here the basic idea and definitions used in spectroscopy calculations.

As usual we form meson and diquark operators by taking correlations of the quark propagator in the appropriate sector of quantum numbers. We shall limit ourselves to the local sector of the spectrum and focus on the zero momentum *connected* propagators of the scalar and pseudoscalar mesons and diquarks. The scalar meson propagator will thus be an isovector, which we will call  $\delta$ , following QCD notation.

By applying a generic O(2f) transformation to the mass term  $\bar{\chi}\chi$  we identify the basic set of operators which shall be used to build the spectrum:

$$\text{scalar} \quad \chi_1\bar{\chi}_1 + \chi_2\bar{\chi}_2 \quad \text{pseudoscalar} \quad \varepsilon(\chi_1\bar{\chi}_1 + \chi_2\bar{\chi}_2) \quad (5.1)$$

$$\text{scalar diquark} \quad \chi_1\chi_2 - \chi_2\chi_1 \quad \text{pseudoscalar diquark} \quad \varepsilon(\chi_1\chi_2 - \chi_2\chi_1) \quad (5.2)$$

$$\text{scalar antidiquark} \quad \bar{\chi}_1\bar{\chi}_2 - \bar{\chi}_2\bar{\chi}_1 \quad \text{pseudoscalar antidiquark} \quad \varepsilon(\bar{\chi}_1\bar{\chi}_2 - \bar{\chi}_2\bar{\chi}_1) \quad (5.3)$$

where the lower index labels colour. The first line displays the usual pseudoscalar and scalar operators. The second (third) line corresponds to diquark (antiquark) operators, scalar and pseudoscalar. This simple minded quantum number assignment can be done by considering that quark – quark and quark-antiquark pairs have opposite relative parity, and is confirmed by a more rigorous analysis presented in HKLM.

Consider now quark propagation from a source at 0 to the point  $x$ . The propagator  $G_{ij}$  ( $i, j$  color index) is an SU(2) matrix:

$$G_{ij} = \begin{pmatrix} a & b \\ -b^* & a^* \end{pmatrix} \quad (5.4)$$

The meson ( $q\bar{q}$ ) and diquark ( $qq$ ) and antidiquark ( $\bar{q}\bar{q}$ ) propagators at  $\mu = 0$  are constructed from  $G_{ij}$  as follows:-

$$\text{pion} \quad \text{tr}GG^\dagger = (a^2 + b^2) \quad (5.5)$$

$$\text{scalar meson} \quad \varepsilon \text{tr}GG^\dagger = \varepsilon(a^2 + b^2) \quad (5.6)$$

$$\text{scalar } qq \quad \det G = (a^2 + b^2) \quad (5.7)$$

$$\text{scalar } \bar{q}\bar{q} \quad \det G^\dagger = (a^2 + b^2) \quad (5.8)$$

$$\text{pseudoscalar } qq \quad \varepsilon \det G = \varepsilon(a^2 + b^2) \quad (5.9)$$

$$\text{pseudoscalar } \bar{q}\bar{q} \quad \varepsilon \det G^\dagger = \varepsilon(a^2 + b^2) \quad (5.10)$$

The notable feature of the propagators at  $\mu = 0$  is the exact degeneracies of the pion, scalar  $qq$  and scalar  $\bar{q}\bar{q}$  and of the scalar meson, pseudoscalar  $qq$  and pseudoscalar  $\bar{q}\bar{q}$ . We then identify two orthogonal directions in the chiral space:

- a)  $\pi$  - scalar diquark - scalar antidiquark
- b)  $\delta$  - pseudoscalar diquark - pseudoscalar antidiquark

All this at  $T = \mu = 0$ .

By increasing the temperature the “Pauli–Gürsey” lattice symmetry is preserved, so the above degeneracies remain true. Chiral condensate is reduced without changing direction, so the six susceptibilities will progressively become degenerate, and there will be no residual Goldstone particle. This behaviour is demonstrated in Fig. 7 where we plot the susceptibilities as a function of  $\beta$ .

The behaviour of the susceptibilities as a function of the chemical potential has been discussed in HKLM. This is suggestive of a rotation in chiral space of the condensate, from the direction “parallel” to  $\langle \bar{\psi}\psi \rangle$  to that “parallel” to  $\langle \psi\psi \rangle$ .

In HKLM we have noticed that “conventional” observables used to monitor chiral symmetry (pion,  $\delta$ , chiral condensate) display a behaviour similar to that observed at finite temperature. While we confirm this finding at qualitative level, we also note a quantitative difference : pion and  $\delta$  become exactly degenerate at high density, while at high temperature a splitting remains – not surprisingly, of course, since the bare mass is not zero. It is the apparent *exact* degeneracy observed for bare masses of comparable value at high density, for both  $\beta$  values, which is sort of puzzling.

The qualitative trend observed at  $\beta = 1.5$  and  $\beta = 1.3$  is quite similar : see Fig. 8, to be contrasted with Fig. 5 of HKLM. In Figs. 9 the susceptibility in the scalar diquark channel is plotted as a function of the bare mass for various chemical potentials at  $\beta = 1.3$  and  $\beta = 1.5$ . It looks as though the signal from the scalar (and pseudoscalar alike) diquark susceptibilities in the chiral limit would be, in any case, much smaller than  $\langle \bar{\psi}\psi \rangle$  at zero chemical potential. It has to be stressed that the meaning of this exercise is simply to check how strong the indication of “rotation” detected with this procedure would be in the chiral limit. In addition to that, there the usual caveats associated with the small lattice size, and poor mass sample apply. These warnings issued, there might well be two effects on the chiral condensate while increasing  $\mu$  : one is indeed a rotation in chiral space, one is a reduction of its magnitude similar to that observed at high temperature.

## VI. THE DYNAMICAL EFFECTS OF THE CHEMICAL POTENTIAL : TWO VS THREE COLORS - SPECULATIVE COMMENTS

To gain further insight into the “dynamical” role of the chemical potential, and its effect on the gauge fields, we can take a look at a Toy [11] version of the model, obtained by inverting the Dirac operator at nonzero chemical potential in a background of gauge fields generated at zero chemical potential. For these configurations the potential is obviously always “hard”, identical to that at  $\mu = 0.0$ . In Fig. 10 we show the scalar diquark propagator for  $\mu = (0, .6, .8)$  evaluated on two different configurations. Interestingly, we have found that in this case the behaviour of the diquarks propagators resembles that of the infamous quenched SU(3) “baryonic pions” measured in [12].

This suggests that the nature of the interquark forces and the deconfinement transition might well play a major role in the condensation phenomena, and thus in the critical behaviour, for SU(2) and SU(3) alike. It is essential to have the correct quark–quark and quark–antiquark forces, since they control and soften diquark condensations, including the pathological ones (which of course should disappear in a correct SU(3) calculation). In a correct QCD algorithm the “baryonic pion” condensation would not take place as the potential become weaker, and the pathological onset at  $m_\pi/2$  would disappear.

## VII. SUMMARY AND OUTLOOK

Our work in this paper stressed those aspects which are instrumental to study the influence of the gauge field dynamics on the phenomena expected at finite baryon density. Temperature dependence is an important tool in this context. A “Toy” model, where the gauge field dynamics is not affected by the chemical potential, proven informative as well.

Although our calculations have not been intended as anything more than exploratory (remember everything was carried out on a  $6^4$  lattice) we feel we have nonetheless managed to learn something from them, which we summarise here.

We have investigated the interquark potential and found evidence of enhanced screening when a nonzero density is induced in the system, as seen in a larger plateau at large spatial separation. We underscore that the plateau builds in is at the onset of the thermodynamics, i.e. when the number density starts deviating appreciably from zero. This supports the results of heavy quarks SU(2) studies that a small density of quarks induces “deconfinement” [13] – these observations are clearly semiquantitative and in particular the nature and the very existence of a nuclear matter state in SU(2) should be subjected to a more careful scrutiny, as discussed in the body of the paper. Temporal and spatial Polyakov loops behave in different ways, the latter being nearly insensitive to the chemical potential, suggesting the expect different spatial and temporal ordering predicted by instanton models. These observations might offer some further insight into Polyakov Loop models [14].

Simple inspection of the heavy quark potential symmetries supports the numerical findings of HKLM, that for any non-zero chemical potential the (rather heavy) particle degeneracies noted at  $\mu = 0$  remain true, once the Fermi level shift is taken into account. This would lead to the four degenerate particles at large chemical potential, when pion and  $\delta$ , and scalar and pseudoscalar diquark, are degenerate. Interestingly, this pattern emerges from a recent model study [15].

The behaviour of the number density changes qualitatively with temperature. Despite the many uncertainties described in the text, it seems anyway clear that screening and deconfinement compete against condensation, and this is better seen on a “warmer” lattice, close, yet below  $T_c$ : there  $n \propto \mu^3$ , consistent with a free, massless quark gas, suggesting the existence of a critical temperature for diquark condensation (i.e. a temperature beyond which diquarks will not condense at any value of the chemical potential) smaller than  $T_c$  itself.

The behaviour of the susceptibilities suggests that there are two effects on the chiral condensate while increasing  $\mu$ : one is a rotation in chiral space, one is a reduction of its magnitude (occurring in the chiral limit) similar to that we have observed at high temperature. The caveats have been spelled out above, and probably only a direct measure of the diquark condensate [9] can clarify this point. Assuming it is confirmed, there are two possible consequences stemming from this observation. In the first place, again, this suggests that there is a critical temperature for diquark condensation: when temperature is high enough the magnitude of the condensate will “shrink” to zero at rather small  $\mu$ , leading to a complete realisation of the chiral symmetry  $\langle \bar{q}q \rangle = \langle qq \rangle = 0$ . Secondly, it could be that this effects ultimately leads to the same complete restoration of chiral symmetry at large density even in the cold phase.

Concerning the comparison of high temperature and high density behaviour, we noticed two interesting, and to our mind puzzling features: while at high density we observe a complete degeneracies among the chiral partners, at high temperature we observe the residual splitting expected of nonzero bare masses; we do not know where this difference –which is numerically quite clear– come from. At the same time, we have not observed any significant difference between the Polyakov loop correlations at large T and large  $\mu$ . Instanton models predict different ordering at large T and  $\mu$  – “instanton-anti-instanton” pairs at high T and “polymers” at high density (see second entry of [4], and [8]) – it would be nice to detect these phenomena in a lattice simulations. This would require more sensitive observables, among which the topological ones, besides lattice instanton studies, seem to be particularly promising. We are now exploring the behaviour of the topological susceptibility, and space – time correlations of topological charge: this should hopefully shed light on these and other relevant aspects [16].

We stress that what has been sketched here constitute a possible coherent scenario *not inconsistent* with the present data, but *certainly not* implied by it. Further studies are necessary to sharpen our understanding and this will certainly require a larger set of chemical potentials and simulations in the scaling region. It is also appropriate to reiterate that according to ref. [17] the theory with two colors and eight continuum flavour should be in the conformal phase, however we have not detected any indication of unconventional behaviour. Either we are too far from the continuum limit, so that the continuum results do not apply, and/or the nature of this new phase is not manifest in our calculation [18]. One the dark side this issues yet another warning on these results, on the bright side this adds to the interest of the model.

A challenging question remains as to whether we can learn anything useful for real QCD. Of course, as two color QCD baryons are completely degenerate with mesons, the system is not a good approximation to real QCD - symmetries and spectrum of two and three color QCD are certainly dramatically different. However there might well be a continuity of the



dynamical effects from  $N_c = 2$  to  $N_c = \infty$ . A good example comes from the behaviour of the diquark coupling [8]. Another from the results of the last section which suggested that similar dynamical effects should take place when going from “Toy” to full dynamics in two and three color QCD. In addition, if we accept that the instanton picture for “real” QCD is correct, and take into account that instantons should be described as configurations belonging to the  $SU(2)$  subgroup of  $SU(3)$  [19], we might even speculate that the two color results would be closer to the real world than expected.

## ACKNOWLEDGMENTS

This paper extends a study initiated in HKLM, and uses the same codes: I wish to thank Simon Hands, John Kogut and Susan Morrison. I also thank: the Zentrum für Interdisziplinäre Forschung, und Fakultät für Physik der Universität Bielefeld; the Dipartimenti di Fisica delle Università degli Studi di Pisa e di Roma I *La Sapienza* for hospitality during various stages of this project. This work was partly supported by the TMR network *Finite Temperature Phase Transitions in Particle Physics*, EU contract no. ERBFMRXCT97-0122.

## REFERENCES

- [1] S.J. Hands, J. B. Kogut, M.-P. Lombardo and S.E. Morrison, hep-lat/9902034, Nucl. Phys. B, to appear.
- [2] J. B. Kogut, Nucl. Phys. B290[FS20] (1987) 1.
- [3] M.E. Peskin, Nucl. Phys. **B175** (1980) 197; S.J. Hands and M. Teper, Nucl. Phys. B347 (1990) 819; J.J. M. Verbaarschot, Phys.Rev.Lett. 72 (1994).
- [4] M. Alford, K. Rajagopal and F. Wilczek, Phys. Lett. **B422** (1998) 247; R. Rapp, T. Schäfer, E.V. Shuryak and M. Velkovsky, Phys. Rev. Lett. **81** (1998) 53; see references therein for earlier work on the subject; these papers have spawned a vaste literature, whose latest developments have been reported in the QCD at finite density reviews by E. Shuryak at LATTICE99, Pisa, and F. Wilczek at PANIC99, Uppsala.
- [5] E. Dagotto, F. Karsch and A. Moreo, Phys. Lett. 169B (1986) 421; E.Dagotto, A.Moreo and U.Wolff, Phys. Lett. **186B** (1987) 395.
- [6] M.-P. Lombardo, in Proceedings of *QCD Phase Transitions*, RIKEN BNL, BNL-52561, p. 38; hep-lat/9906006, to appear in Proceedings of *Understanding Deconfinement in QCD*, Ect\*, Trento.
- [7] I thank Dirk Rischke for pointing this out.
- [8] R. Rapp, T. Schäfer, E.V. Shuryak and M. Velkovsky, hep-ph/9905353.
- [9] S. J. Hands and S. E Morrison, hep-lat/9905021, to appear in Proceedings of *Understanding Deconfinement in QCD*, Ect\*, Trento.
- [10] W. Bietenholz and U.J. Wiese, Phys.Lett. B426 (1998) 114.
- [11] I. M. Barbour, S.J. Hands, J. B. Kogut, M.-P. Lombardo and S.E. Morrison, hep-lat/9902033, Nucl. Phys. B, to appear.
- [12] M.-P. Lombardo, J.B. Kogut and D.K. Sinclair, Phys.Rev. D54 (1996) 2303.
- [13] K. Langfeld and G. Shin, hep-lat/9907006.
- [14] M. Plewnia, I.O. Stamatescu and W. Wetzel, Nucl. Phys. B (Proc. Suppl.) 26 (1992) 323; T. C. Blum, J.E. Hetrick and D. Toussaint, Phys. Rev. Lett. 76 (1996) 1019; J. Engels, O. Kaczmarek, F. Karsch and E. Laermann, hep-lat/9903030; Ph. de Forcrand and V. Laliena, hep-lat/9907004.
- [15] J.B. Kogut, M.A. Stephanov and D. Toublan, hep-ph/9906346.
- [16] B. Allés, M. D’Elia, M.-P. Lombardo and M. Pepe, in preparation.
- [17] T. Appelquist and F. Sannino, Phys.Rev. **D59** (1999) 067702.
- [18] Interesting suggestions on signatures of the conformal window amenable to lattice calculations are in V. A. Miransky, Phys. Rev. **D59** (1999) 105003.
- [19] A. Di Giacomo, Acta Phys.Slov. 49 (1999) 159, and references therein.

# FIGURES

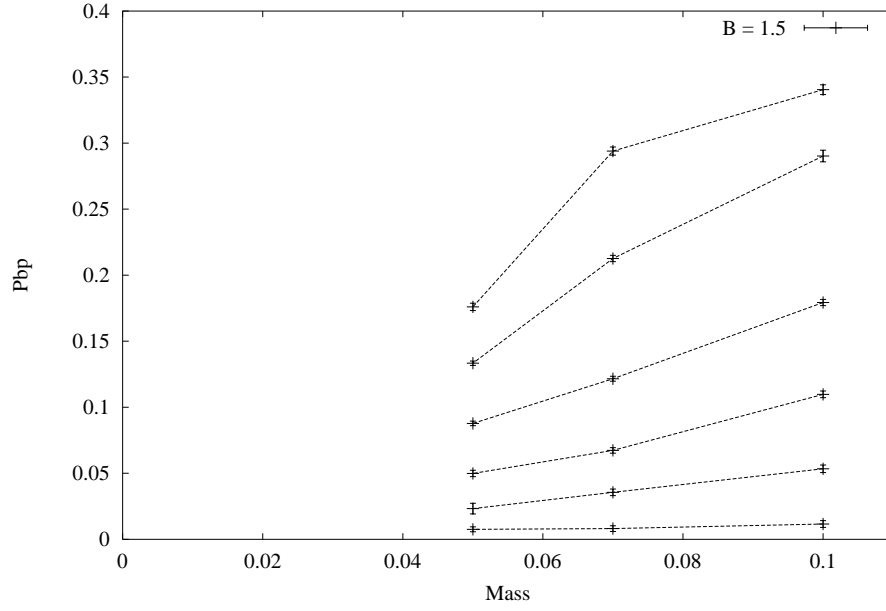


FIG. 1.  $\langle \bar{\psi}\psi \rangle$  as a function of the bare mass,  $\beta = 1.5$   $\mu = 0, .2, .4, .6, .8, 1.0$  from top to bottom

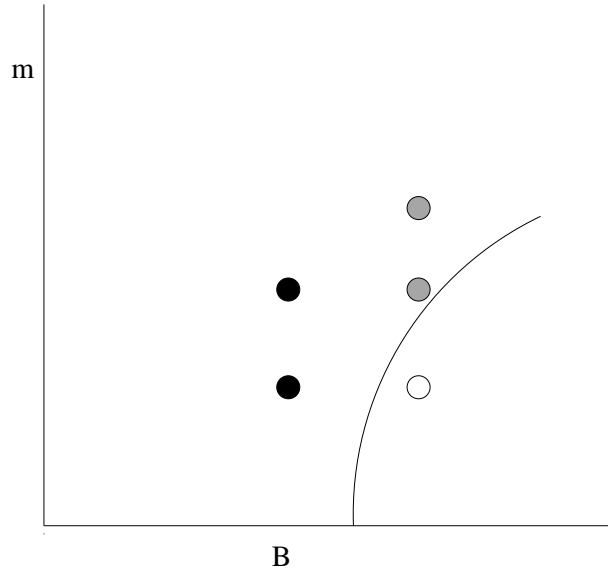


FIG. 2. The critical line in the  $\beta$ -mass plane and the simulation points at  $\beta = (1.3, 1.5)$ , mass=(.05, .07, .1)

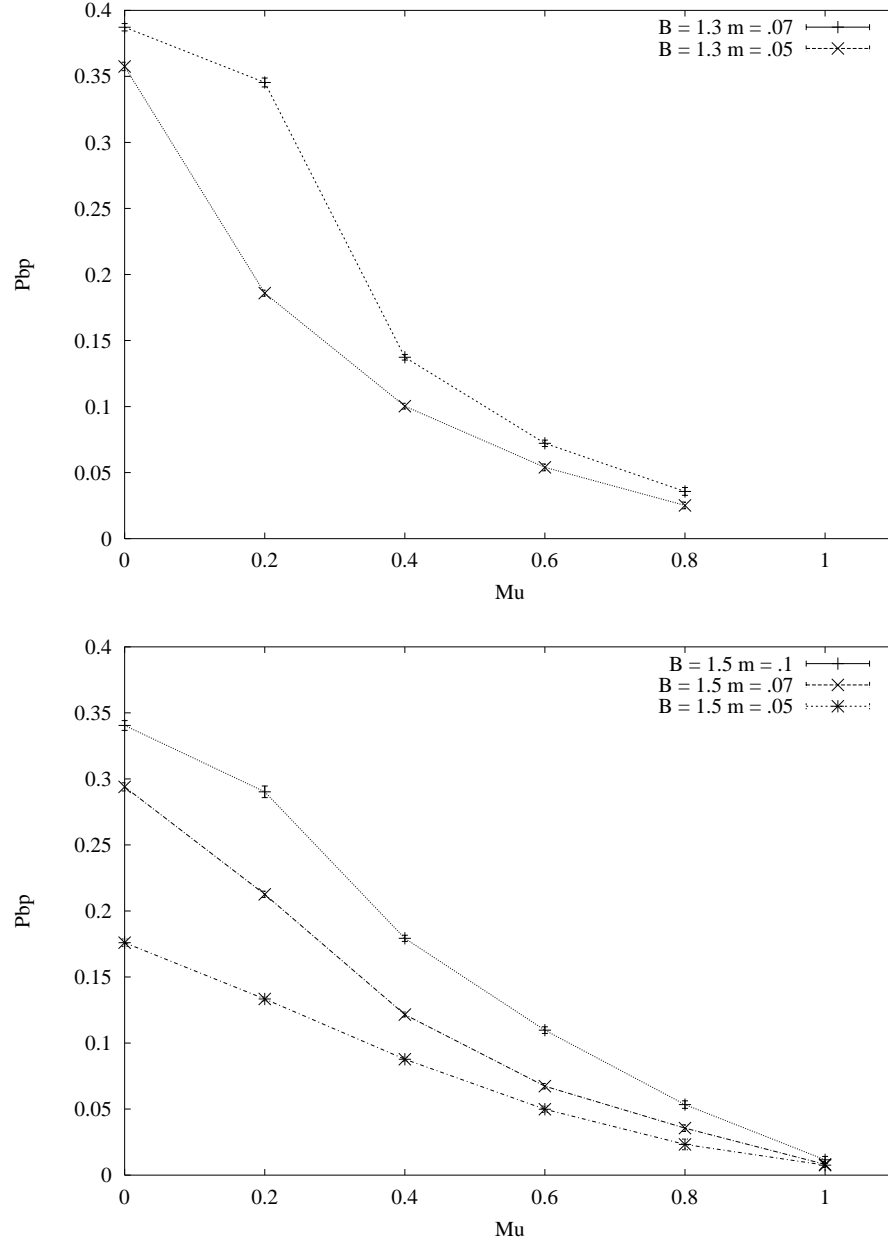


FIG. 3.  $\langle \bar{\psi}\psi \rangle$  as a function of the chemical potential for  $\beta = 1.3$  (upper, reproduced from HKLM) and  $\beta = 1.5$ , and masses as shown in the diagrams

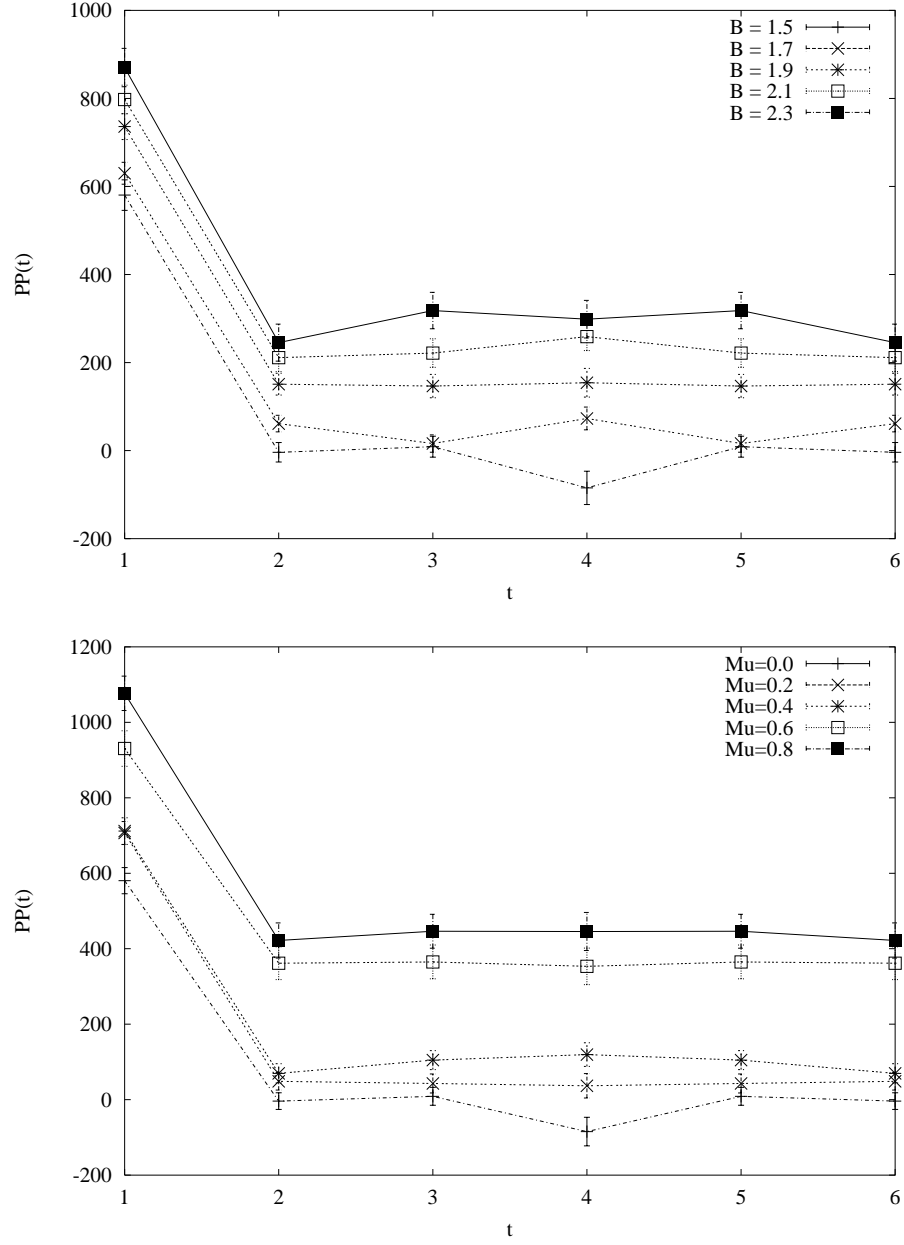


FIG. 4. Correlations of the zero momentum Polyakov loop as a function of the space separation. The upper diagram is for  $\mu = 0$ , and  $\beta$  as indicated. The lower part is for  $\beta = 1.5$  and  $\mu$  as indicated. In both cases we observe long range ordering possibly associated with deconfinement

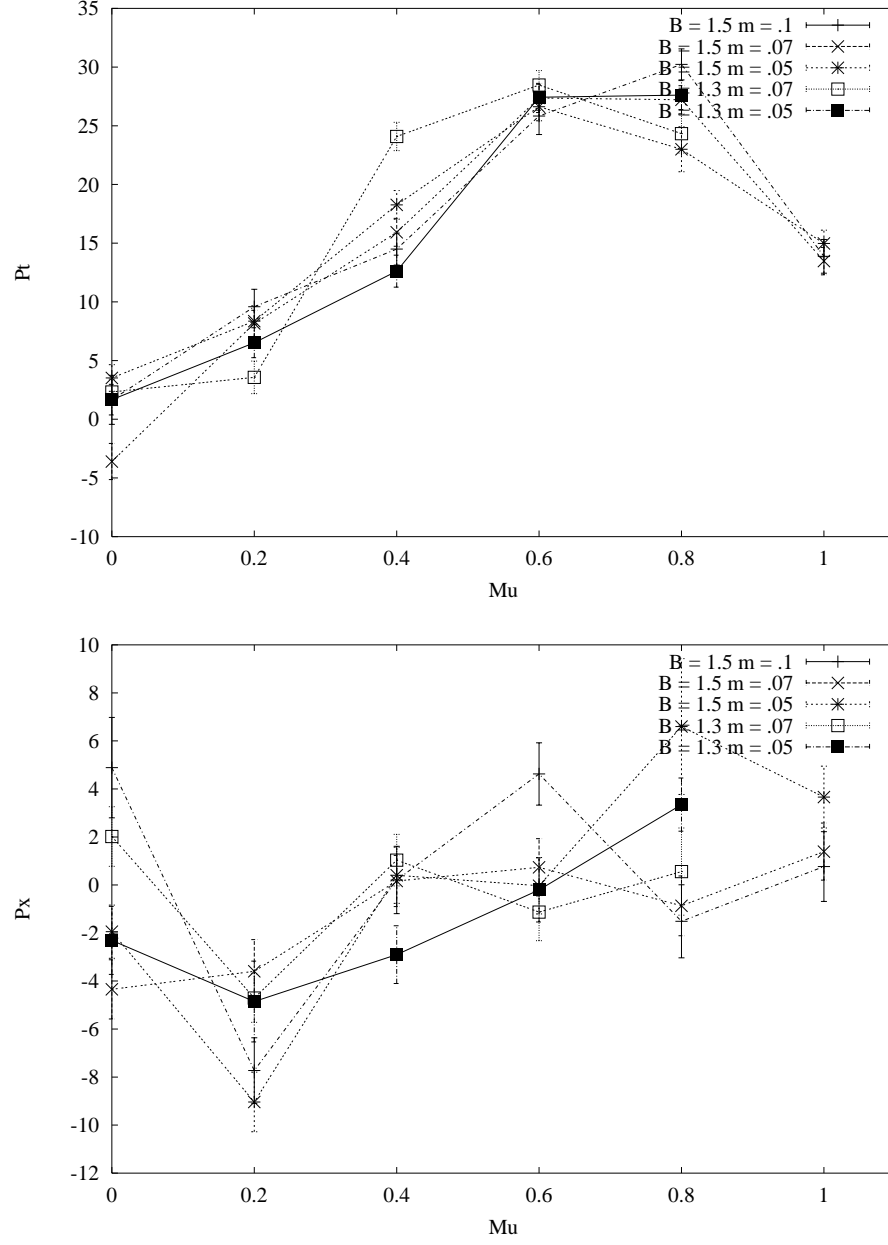


FIG. 5. Polyakov loops as a function of the chemical potential. The upper diagram is for the temporal Polyakov loops, the lower diagram for one spacial direction (the others behave similarly)

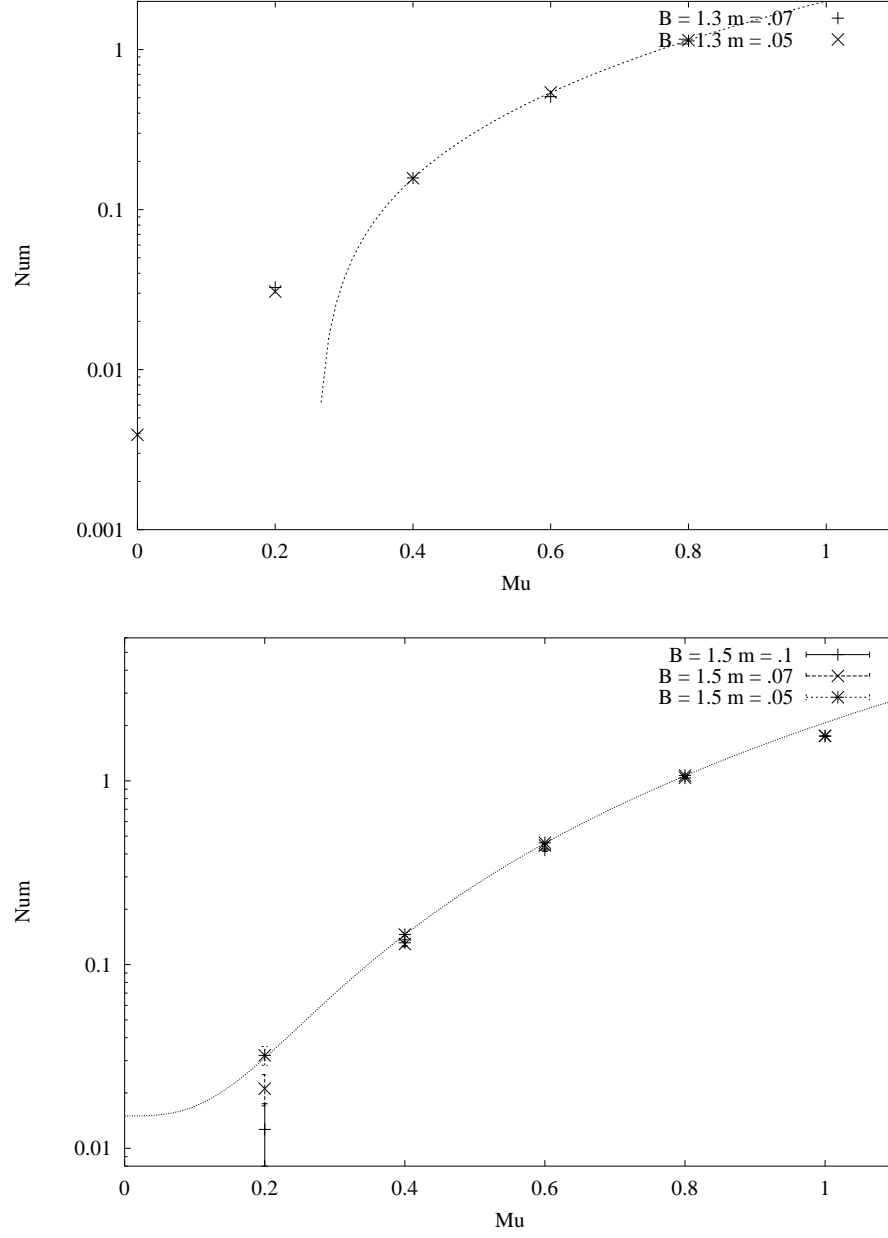


FIG. 6. Number density as a function of the chemical potential, for different masses. The cubic fits to  $a\mu^3 + b\mu^2 + c$  are superimposed.  $b, c \simeq 0$  for  $\beta = 1.5$  : the behaviour is then consistent with a pure quark gas.

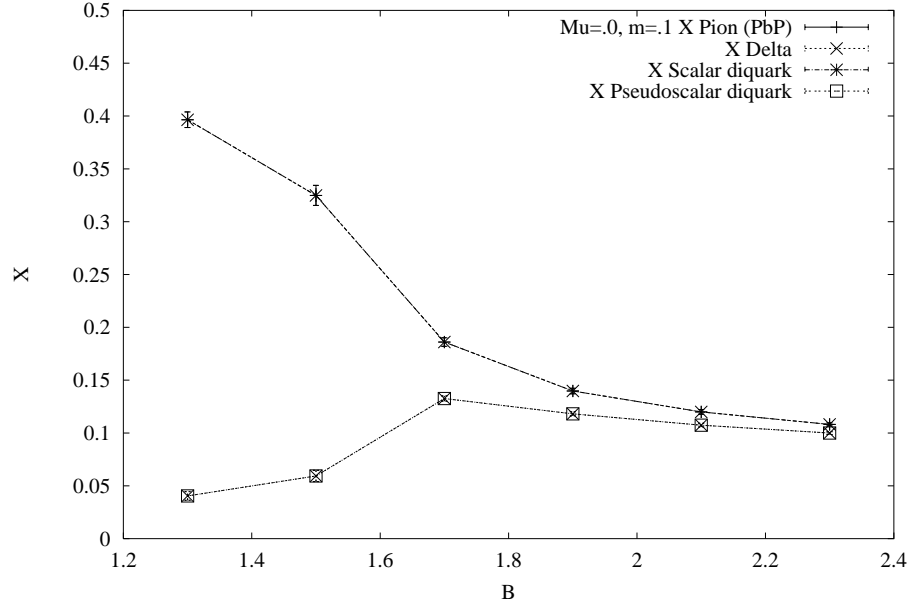


FIG. 7. Scalar and pseudoscalar susceptibilities as a function of  $\beta$  demonstrating chiral symmetry restoration at high temperature



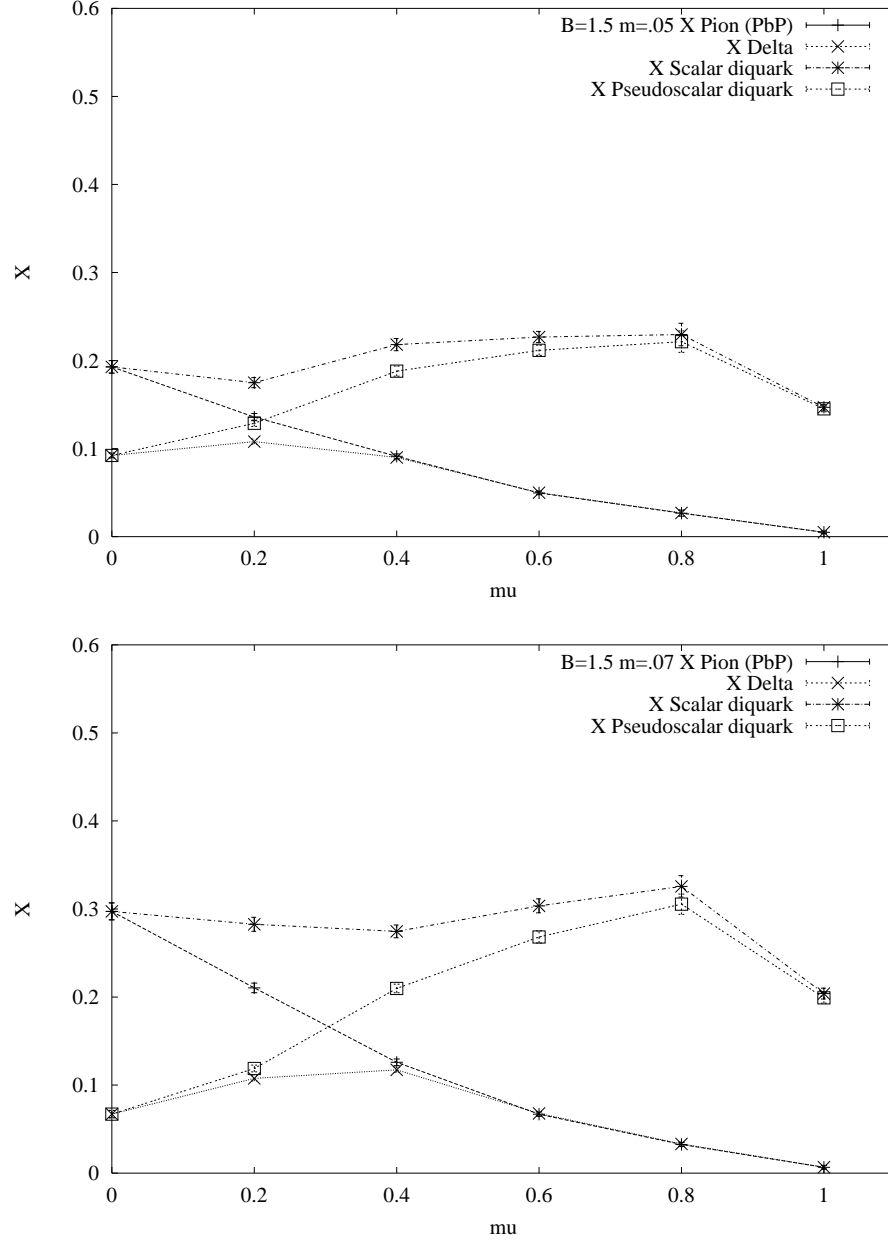


FIG. 8. Scalar and pseudoscalar susceptibilities for mesons and diquarks a function of  $\mu$  at  $\beta = 1.5$  and mass = .05 (upper) and mass = .07. See text for discussions

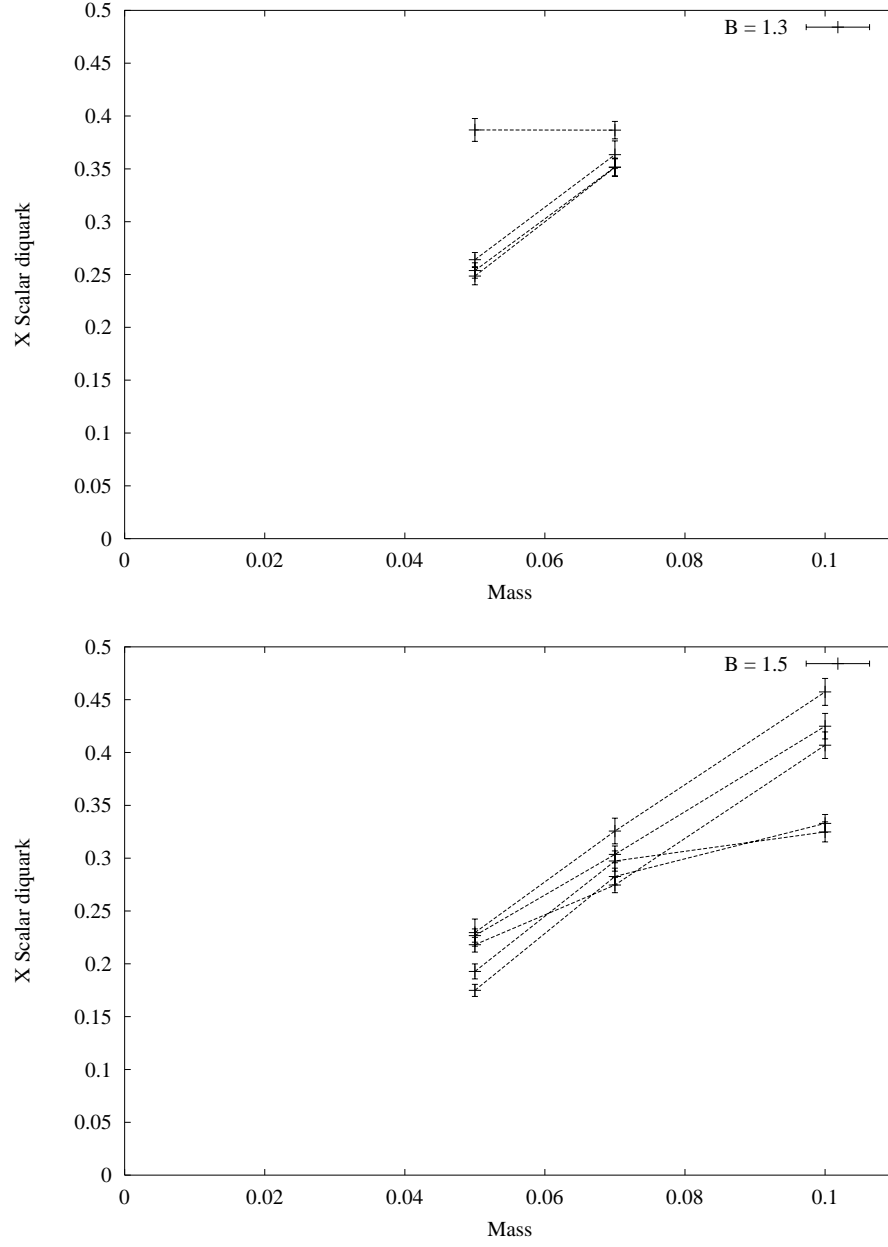


FIG. 9. Scalar diquark susceptibilities as a function of mass for various  $\mu$  at  $\beta = 1.3$  and  $\beta = 1.5$

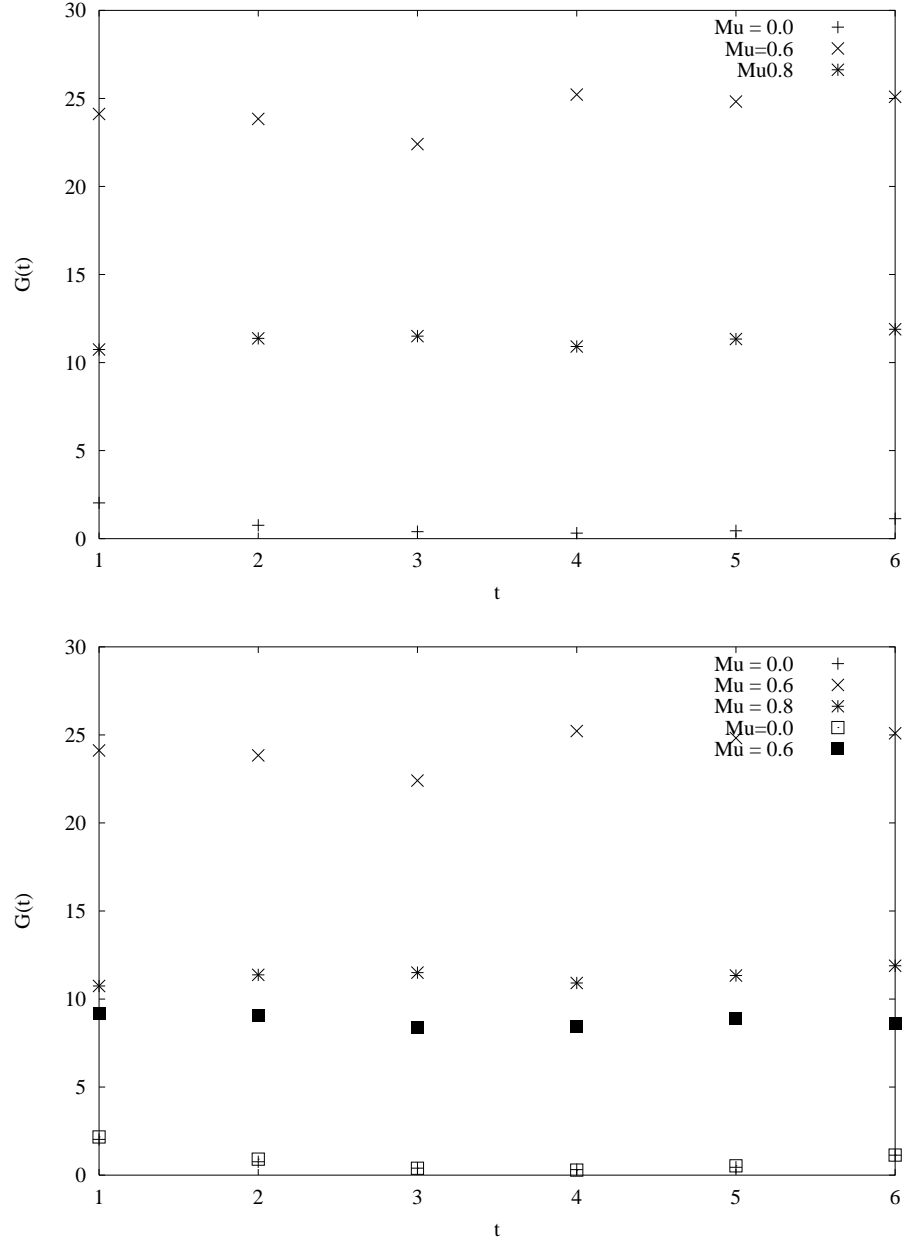


FIG. 10. Strong diquark condensation in the Toy model on two different configurations. These two configurations have been generated at  $\mu = 0$ . The Dirac propagators have been calculated with the chemical potential indicated in the diagrams.